5 Measures of CT Scanner Performance

The main factors that determine the imaging capabilities of a CT scanner used in engineering applications are its achievable spatial, temporal and density resolution. The spatial resolution of any imaging system is defined as the minimum distance that two high contrast point objects can be separated by, in order for the imaging system to perceive them distinctly. A measure of the spatial resolution is the point spread function (PSF) which is the extent to which the image of a point object would be blurred. The width of the PSF at half its maximum value, known as full-width-at-half-maximum (FWHM), is the criterion most commonly used for specifying the resolving power of an imaging system (Glover and Eisner, 1979). It should be noted that two PSF's may have the same FWHM but different shapes and, therefore, in specifying the resolution it is necessary to indicate the complete PSF rather than just the FWHM. For most imaging systems the PSF is a function of position and may vary from the center to the periphery of the image. It is however, desirable to have an approximately isotropic PSF and this is often achieved in well designed CT scanners. A simple method of measuring the PSF of a CT scanner is to image a phantom consisting of an object that is dense and narrow (eg. a thin steel wire) that is positioned perpendicular

to the imaging plane. Imaging a number of such infinitesimal point objects interspersed at several locations in the plane would enable the determination of the variation in the PSF. The most significant factors that affect the PSF of a CT scanner are geometric factors, and the reconstruction algorithm. The geometric factors that affect the resolution are the focal spot size of the X-ray tube (the size of the isotope for a γ ray source), the aperture of the detectors, the magnification factor and the spatial sampling rate. The magnification factor is the ratio of the focal spot-detector distance to the focal spot-object distance. Since in practice both the focal spot and the detector aperture are finite, the region subtended between the two is trapezoidal as shown in Fig. 8a. The measured attenuation profile of an elementary object depends on the position of the object within the trapezoidal region. Assuming a uniform focal spot intensity distribution, and a uniform detector response, the measured attenuation profile of the elementary object is either trapezoidal, or triangular as shown in Fig. 8b. Thus, the image of a point object is broadened by the finite width of the focal spot and the detector aperture. A measure of this blurring in terms of the dimensions

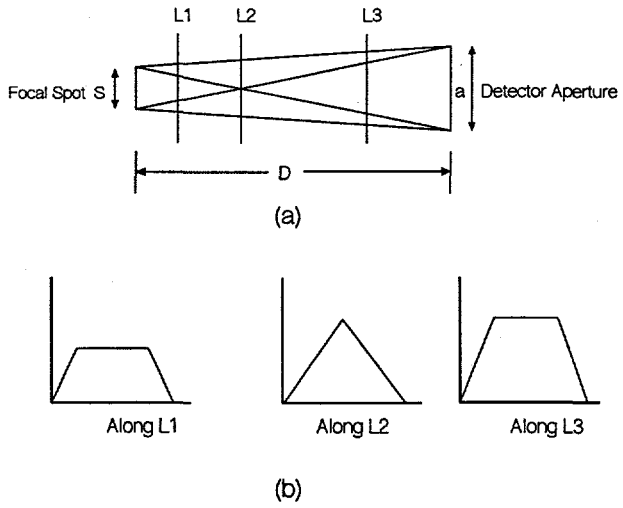

Figure 8: (a) Geometry for attenuation profiles at different positions between the source and detector; (b) Attenuation profiles for an elementary point object at different points along the trapezium

of the focal spot size s, the detector aperture d_a and the magnification factor M has been derived by Yester and Barnes (1977) as :

$$d_{eff} = \frac{1}{M}\sqrt{d_a^2 + (M-1)^2 s^2} \tag{10}$$

where d_{eff} is the effective detector aperture width, which is related to the approximate width of the blurred image of the point. This expression dictates that the focal spot and the detector aperture be reduced in order to reduce the FWHM of the PSF. For purposes of providing an adequate area for photon detection in order to have faster data acquisition rates it is desirable to have a large detector aperture. Hence, there needs to be some compromise between the two conflicting requirements. In addition, the PSF is also dependent on the frequency of spatial sampling. The interaction between the various parameters affecting spatial resolution has been investigated comprehensively by Yester and Barnes (1977). Their results indicate that the spatial sampling interval need be no smaller than the focal spot size. In fact, a degradation of the PSF is seen with increase in the spatial sampling frequency. More on the requirements of spatial sampling will be discussed in connection with aliasing artifacts.

The temporal resolution refers to the frequency with which the images can be obtained. For process systems it is desirable to have the measurements completed rapidly so that the time evolution of the flow phenomena can be studied. With X-ray and gamma ray tomography the data obtained for the concentration distribution of phases is almost always time averaged, since it generally requires a significant period of time to obtain the photon count rates for all the projections in a significant number of views with good photon counting statistics. Depending on the design of the scanner this period can range anywhere from a few minutes to close to an hour. This is a basic limitation of X-ray and gamma ray tomography with the scanner designed with the fan-beam scanning geometry. With the recent advent of impedance tomography techniques it has become possible to obtain time resolved measurements, since in these systems there is no need for physically rotating the sensors and the source, as is required in X-ray and gamma ray CT systems.

The density resolution of a CT system refers to the smallest difference in mass attenuation coefficients that the system is able to distinguish. The standard deviation of the statistical distribution of the density in each pixel based on a constant object cross-sectional density of $1\,g/cm^3$ can be used as a measure of the density resolution of the system. The single important factor that determines the density resolution is the random fluctuations in the photon counts delivered by the X-ray tube or the gamma ray source. This is because the difference in photon counts caused by a difference in mass attenuation coefficient of the materials in the path of the beam has to be significantly higher than the fluctuations in the photon count rate. The higher the intensity of the radiation, the smaller is the standard deviation of the photon count rate and the better the density resolution is. Having a higher intensity of radiation is, however, not desirable owing to safety considerations.

Different authors have derived different expressions for a quantity that serves as a measure of the density resolution that accounts only for photon counting statistics. Shepp and Logan

(1974) have derived the following expression for the density resolution :

$$\sigma^2 = \frac{4}{I_d \, (log \, \frac{I_d}{I_e})^2} \tag{11}$$

where I_d and I_e are the number of detected and emitted photons, respectively. De Vuono (1979) has derived an expression for the density resolution obtainable from all the measurements in an entire scan as follows :

$$\frac{\sigma_\rho}{\rho} = \frac{n}{2 \, \mu_w \, \rho_w \, d_i \, \sqrt{m \, N}} \tag{12}$$

where n is the number of beams in each view, m is the number of views, N is the average number of photons detectable per beam, μ_w is the mass attenuation coefficient of water and ρ_w is the density of water. The above expression involves a constant that has been set to 0.5.

It is clear from the above expressions that improvements in density resolution can be obtained by increases in the number of views obtained in the scan as well as by an increase in the number of detected (and hence the emitted) photons. Any increase in the number of views increases the scanning time. With X-ray tubes it is relatively easy to improve upon the count rates since it is just a matter of increasing the input voltage to the tube. This, however, is not the case with gamma ray sources since the emission rate of photons is fixed by the source activity and decay rate. In order that the reduction in photon count rate due to radioactive decay is not significant during the scanning process, isotopes with a significantly large half-life have to be used.

6 Sources of Error in CT Scanning

The process of CT scanning from measurement of the photon count rate to final reconstruction and display of the image is subject to a set of problems that lead to artifacts or errors in the final result. Some of the problems that can arise include misalignment in the hardware configuration, noisy measurements, and sometimes a poor choice of the reconstruction algorithm and its parameters.

The following is a list of possible sources of error in the experimental procedure from scanning to final reconstruction :

- Geometric misalignment artifacts
- Statistical uncertainty in photon counts
- Compton scattering effects

- Beam hardening effects
- Data sampling frequency in space
- Dynamic bias or void fluctuation effects
- Errors in the image reconstruction process
- Errors and variations in detectors and source

Geometric misalignment artifacts

The mechanical components of a CT scanner need to be well designed to provide great precision and accuracy in the positioning of the detector array and the source of radiation with respect to the test section. Most often it is difficult to ensure that the mechanical center of rotation coincides with the center of the coordinate system used in the reconstruction process. This leads to an incorrect calculation of the contribution of the projections to the pixels that are not truly in the beam path. The problem is especially serious in systems that make use of algorithms that involve the backprojection process such as the Filtered Back-projection algorithm. This calls for accurately locating the center of rotation of the system. This is rather problematic since physical measurements are prone to error. For the CT scanner in our laboratory this measurement has been made within a range of $\pm 1\, mm$ and this, coupled with the use of the E-M algorithm that does not make use of the back-projection process, appears to provide reasonably accurate reconstructions. Instead of making an accurate measurement of the center of rotation Azevedo et al. (1990) suggest the determination of the center from the reconstructed image of a simple phantom by adopting a least squares technique. It is based on the principle that the center of mass of the object projects into the center of mass in each view. The method determines the center of rotation based on the least squares sinusoidal fit to the row wise centers of mass in the reconstructed image. The claim is that this is a robust method that matches experimental measurements as long as noise levels in the image are not high.

Uncertainties due to the Statistical Nature of the Source

Statistical noise in CT images arises out of the random fluctuations that occur in the counting of photons. This is an inherent limitation of the process and the relative accuracy of measurement can be increased only by an increase in the number of detected photons. Another measure that is adopted is to consider the average of a series of samples as a single measurement. Thus, the number of photons obtained for a projection are taken to be the mean of N observations. If $\overline{C_n}$ denotes the mean number of counts, then Barret (1974) specifies that the following criteria need be satisfied for reducing the error due to counting and source fluctuation effects : N is large; $\overline{C_n} \gg 1$ and $1/\overline{C_n^2} \ll 1$. An increase in the number of detected photons, however, is in contradiction to the requirements of reducing the

exposure from radiation due to safety consideration, and averaging a series of samples leads to an increase in the scan time. Optimum source strengths (or X-ray tube output) and a reasonable number of samples have to be found for each application. The CT scanner in our laboratory makes use of a Cesium-137 source of 100 mCi activity, and each measurement is taken to be the average of 54 samples obtained at the rate of 10 Hz, so that each projection measurement is averaged over a period of approximately 6 seconds.

Compton Scattering Effects

The interaction of radiation (X-ray or gamma ray) with matter can be either in the form of attenuation or in the form of scattering. With attenuation a photon is considered to be removed from the beam of radiation completely. In Compton scattering on the other hand, the photons are not removed from the beam but instead have a lower energy than before and their direction of travel is also altered. The Beer-Lamberts' law can be used for the measurement of holdup only in the presence of attenuation. However, the probability of detecting a scattered photon along with the unattenuated photons in a beam is non-zero and this leads to an attenuation coefficient that is lower than the actual value. To minimize the errors due to Compton scattering it is necessary to take into consideration only those photons that are at or near their unattenuated energy level. The ideal way to approach the problem is to use a multi-channel analyzer that not only counts the photons but also provides a measure of the associated energy. However, it suffices to make use of a discriminator that produces a logic pulse only for those unscattered photons depositing their full energy in the detectors. In addition, the probability of detecting a scattered photon is reduced by collimating the beam. The detectors are provided with collimators made of lead or tungsten, or even steel, which are about 2 to 3 inches deep. The width and height of the opening are designed on the basis of the required spatial resolution, the spatial sampling interval and the available photon flux. Thus, due to collimation, scattering is much less of a problem in systems with second and third generation scanning configurations. In fourth generation machines each detector, unlike in the other configurations, needs to accept radiation from a range of angles of incidence making scatter rejection by collimation impossible. In this scanning configuration collimation is provided only along the axial direction so that only those photons that are travelling in a narrow plane are detectable. Swift et al. (1978) have derived the following relation for the measured transmission ratio accounting for the effects of low angle forward scattering of photons:

$$I/I_\circ = e^{-\mu l} + \frac{1}{2}\left(\frac{d_a}{x_d}\right)^2 (1 - e^{-\mu l}) \tag{13}$$

where the second term on the right hand side accounts for the scattering effects. d_a and x_d are the detector aperture and the distance of the scattering event from the detector, re-

spectively. For the scanner that was implemented in the authors' laboratory the detector aperture is 5 mm and for the worst case scenario x_d can be only as small as 98 mm, so that the term which determines the extent of the scattering contribution works out to be $0.001307(1 - e^{-\mu l})$ and is very small in comparison to $e^{-\mu l}$.

Beam Hardening Effects

In general the Beer-Lamberts' law for the attenuation of radiation is applicable only for monochromatic emissions from the source of radiation. The radiation from any source is polychromatic, that is to say that the source emits photons of different energies. Consequently, in the passage of a beam of radiation through some material the lower energy photons get attenuated earlier than the higher energy photons and, consequently, the spectrum of the emerging radiation is different from the one that is entering. This makes the object more transparent then it really is (the density is under-estimated) leading to what is referred to as beam hardening artifacts. Beam hardening effects are important only in situations where the spectrum of the source emissions is wide (with two or more peaks) and the object being scanned has materials having vastly different attenuation coefficients like bone and tissue. One of the prime considerations in selecting the radioactive source is, therefore, that its emission spectrum be as narrow as possible, and Cs-137 satisfies this requirement extremely well. X-ray tubes generally provide photons with a significant distribution of energy. The flow structure of multiphase systems do not exhibit the same high gradients in density as is typically encountered in scanning the human head. In these systems a more gradual and often monotonic variation in concentration distribution of the phases is expected. Furthermore the magnitude of the differences in mass attenuation coefficients of the materials involved in flow systems is not as large as in the case of human head (bone and tissue). Consequently, it is reasonable to neglect the effects of beam hardening provided the energy spectrum of the photons has a narrow distribution.

Frequency of Spatial Data Sampling - Effects of Aliasing

The spatial interval with which the projections are required to be sampled depends on the frequency content of the object. The Nyquist theorem states that signal sampling should be at a frequency that is at least twice the maximum frequency present in the system being studied. Thus, if ω is the maximum frequency that is contained in the frequency components of the object, then the projections must be spaced at intervals of $\frac{1}{2\omega}$. However, since there is no a priori information about the flow system, this rule is not convenient to determine the fineness with which the projection measurements are to be made. For a chosen sampling interval the consequence of the object containing frequencies higher than the Nyquist limit is that the information content of the higher frequency components masquerade as those

corresponding to some lower frequency components, and hence the name *aliasing.* It is, therefore, necessary to eliminate all spatial frequencies higher than the Nyquist limit by a filtering operation. With CT scanners the width of the sampled beam itself acts as a filter removing frequencies greater than $1/d_a$ before the sampling process. Thus, aliasing artifacts can be reduced by the proper selection of the beam width (detector aperture). Increasing the beam width, as was discussed earlier, sacrifices the achievable spatial resolution.

The fact that the effects of aliasing are not a serious problem for imaging concentration distribution in multiphase systems is demonstrated with some data obtained with the CT scanner in our laboratory. It has already been described in an earlier section that in this scanner each detector is made to sample 8 beams which works out to angular increments of 0.5° within the fan beam. This spatial sampling interval has been demonstrated to be adequate for the measurement of the holdup distribution in a gas-liquid bubble column. The

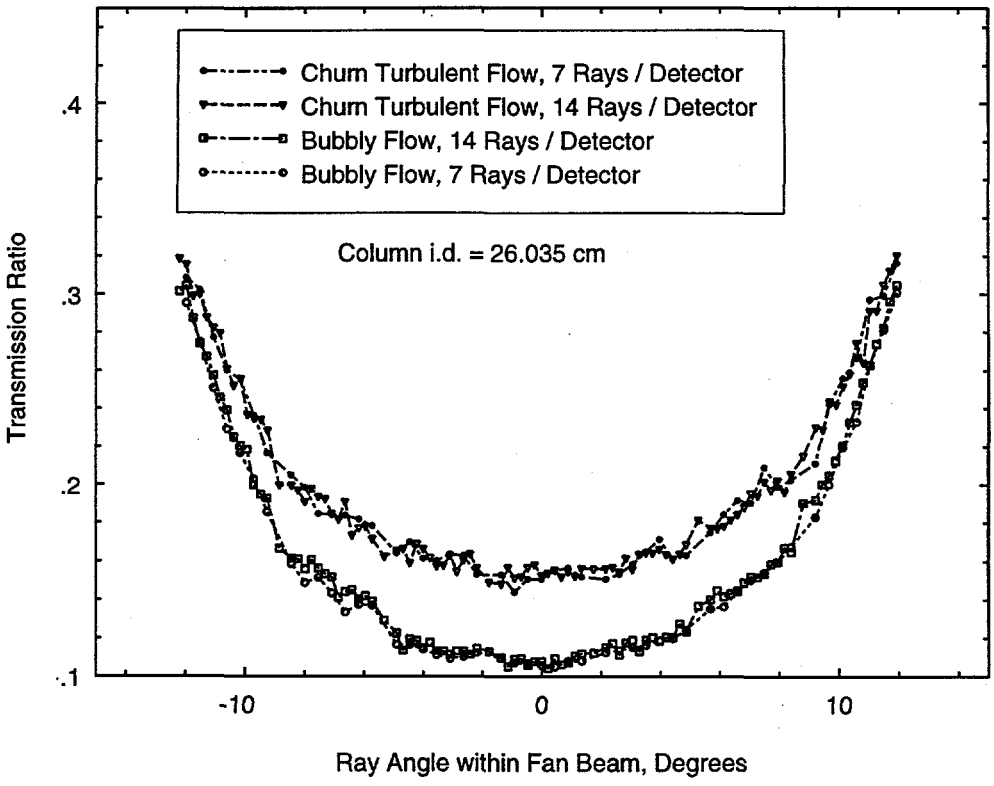

Figure 9: Effects of increase in the frequency of spatial sampling of projections.

bubble column diameter is 0.26 m and the projection measurements were obtained by sampling at the above mentioned frequency as well as twice that rate (i.e., at angular increments of 0.5° and 0.25° in the fan beam) for operating conditions that correspond to bubbly and churn turbulent regimes. The measurements were used to compute the transmission ratio

as a function of angular position within the fan beam. The results are illustrated in Fig. 9, where the data corresponding to both sampling rates have been superimposed for the chosen operating conditions of the bubble column. It is observed that essentially no additional information is gained when the projections are sampled at the higher rate. It is expected that this holds true for other multiphase systems, such as gas-solid and gas-solid-liquid systems.

Dynamic Bias or Void Fluctuation Effects

An error that is unique to the probing of two phase flows by radiation techniques is the one associated with dynamic biasing. This arises from the stochastic nature of the emissions from a gamma ray source and the temporal variations of the void fraction. An error free measurement is possible only in the case of a constant source and static void fraction, both of which are not realizable. Because of the exponential attenuation of the radiation traversing a medium, the logarithm of a time averaged measurement is not equal to the time average of the logarithm of the measurement. If the time over which the averaging is performed is small, then the variation in the void fraction within that time interval is small and the static void approximation is valid. On the other hand, the longer the time allowed for the photon counting, the smaller is the error in the counting process due to the statistical nature of the emissions from the source. Most often the sampling time for each projection is adequate to provide good statistics in the photon counting process. The question that remains is whether the void structure is constant within this period of time. Wyman and Harms (1985) have made a thorough theoretical analysis of this aspect and specify the following relation for selecting the observation interval length :

$$t_{obs} = \frac{\lambda \, t_f \, \alpha}{u(\lambda, \delta)} \tag{14}$$

where t_{obs} is the optimum sampling period, λ is a factor depending on the size of the test section and the mass attenuation coefficient of the medium in the test section, α is the allowable error in void fraction, t_f is a characteristic time of the fluctuations in the flow, δ is the amplitude of the fluctuations in the voids about the mean and u is a function of λ and δ. Unfortunately, neither δ nor u are known a priori preventing the determination of t_{obs} by this equation for a given flow system. Consequently, the time for sampling each projection measurement was determined for the CT scanner in our laboratory by adopting the simpler approach suggested by Barret (1974). A counting experiment is performed over a long period of time, recording on a time scale the positions at which each count occurs. The effective mean for the whole period is computed. The record of counts over the period is split into a number of subperiods each of duration δt, and the effective mean for that interval is found. This process is repeated for smaller and smaller intervals taking care that the interval is not

made too small for statistical counting errors to arise. The means corresponding to each of the sub-intervals are examined for convergence with respect to the mean for the single long time interval. This simple experiment was done for the flow in an air-water bubble column of 0.27 m in diameter, both at bubbly (U_g = 0.02 m/s) and churn turbulent flow conditions (U_g = 0.08 m/s), and the chordal void fraction was computed for a few detectors. The results are presented in Table 3 for some arbitrarily chosen rays in the fan beam. The measured chordal void fraction appears to be independent of the sampling period for the tested flow conditions (representative of most flows). Consequently, a sampling period of 0.1 sec was considered to be sufficiently small for making the static void fraction approximation.

Table 3: Measured chordal void fraction for different sampling periods

Flow Regime	Sampling Period	Chordal Void Fraction at		
	- secs	0.0°	−7.08°	10.58°
Bubbly Flow	0.1	0.084	0.098	0.080
	0.05	0.084	0.099	0.086
	0.03	0.084	0.102	0.088
Churn Turbulent Flow	0.1	0.250	0.250	0.030
	0.05	0.245	0.258	0.030
	0.03	0.250	0.260	0.032

Errors in Image Reconstruction

In scanners that make use of the Filtered Backprojection algorithm the choice of the filter and its cutoff frequency has a significant impact on the final reconstructed image. The common filters that are used in practice are the Ramp, Hann, Hamming and Parzen (Stanley, 1975). A parameter that is to be set for any such filter is its cutoff frequency. If it is desired to retain high frequency information, then the cutoff frequency is set to a high value. However, it is the high frequency components that are the most susceptible to contamination by noise. Therefore, the noise gets amplified and leads to artifacts referred to as streaks. Schneberk et al. (1990), have studied the effect of the choice of windows and the cutoff frequency on the reconstruction of a point object. Their results indicate that the ramp filter provides the best edge detection (detection of sharp features) capability but at the cost of higher noise amplification. The Parzen filter on the other hand is seen to suppress noise effects but leads to a higher FWHM for the PSF i.e., the spatial resolution is sacrificed. The other two filter

windows are said to provide a performance that is in between the above two. For the imaging of multiphase flow systems the choice of the filter may not be too critical mainly because the information content in the distribution of phases is such that they are identified under any filtering scheme. In addition, the achievable resolution is probably limited by the hardware constraints rather than the choice of filter for reconstruction by the Filtered Backprojection algorithm. For the Algebraic Reconstruction Techniques (ART) and the E-M algorithm there is no parameter such as the cutoff frequency of a filter. The accuracy of reconstruction from these algorithms mainly depends on the accuracy of the measurements, and the accuracy with which the geometry of the data collection with respect to the coordinate system for image reconstruction can be provided as input.

The accuracy of image reconstruction by the E-M algorithm is demonstrated by reconstructing the images from simulated and measured projections of static objects. For both the simulation and measurement a plexiglas column with 0.19 m internal diameter and a wall thickness of 0.635 cm filled with water was considered. The data was simulated using 39 projections per view, and there were 90 such views collected over 220°. The scanner in our laboratory was programmed to get the data in the same manner. The reconstruction was done on 36 $\times$ 36 grid for a spatial resolution of 0.54 cm. Ideally, the reconstruction should yield a value of 0.086 cm^2/g in all the pixels, the value corresponding to the mass attenuation coefficient of water at 660 keV which is the peak photon energy of the Cesium-137 isotope. Figures 10 (a) and 10 (b) are the plot of the histograms for the spread of the reconstructed pixel values for the simulated and actually measured data, respectively. The mean and standard deviation of the reconstructed pixel values for the simulated data are 8.65×10^{-2} and 2.51×10^{-3}, respectively. The corresponding quantities for the measured data are 8.73×10^{-2} and 3.73×10^{-3}, respectively. The spread for the simulated data is narrower leading to the conclusion that provided the measured data is accurate the E-M algorithm provides reasonably accurate reconstructions.

Errors and Variations in Detectors and Source

Variations and defects in the detectors or the source of radiation cause errors in the projection measurement. A single detector, and its corresponding data acquisition channel, may be malfunctioning and lead to erroneous measurements in either a single or a set of projections depending on the scanning configuration. In a scanner of the third generation type a defective detector would lead to an incorrect, or a set of incorrect, projections in all the views of the object. This particular beam or set of beams, is tangent to a circle in the image plane and would lead to what is known as ring or circular artifact. With fourth generation scanning a single defective detector leads to all the projections in one view to be in error. The resulting error in reconstruction is far less serious than the ring artifact because it is

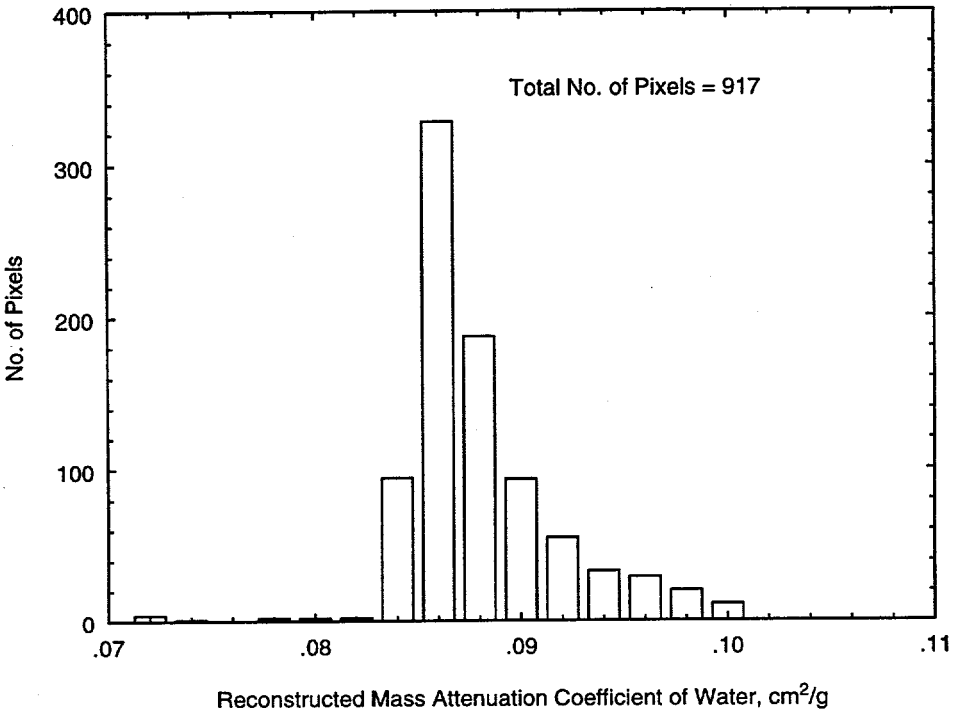

(a)

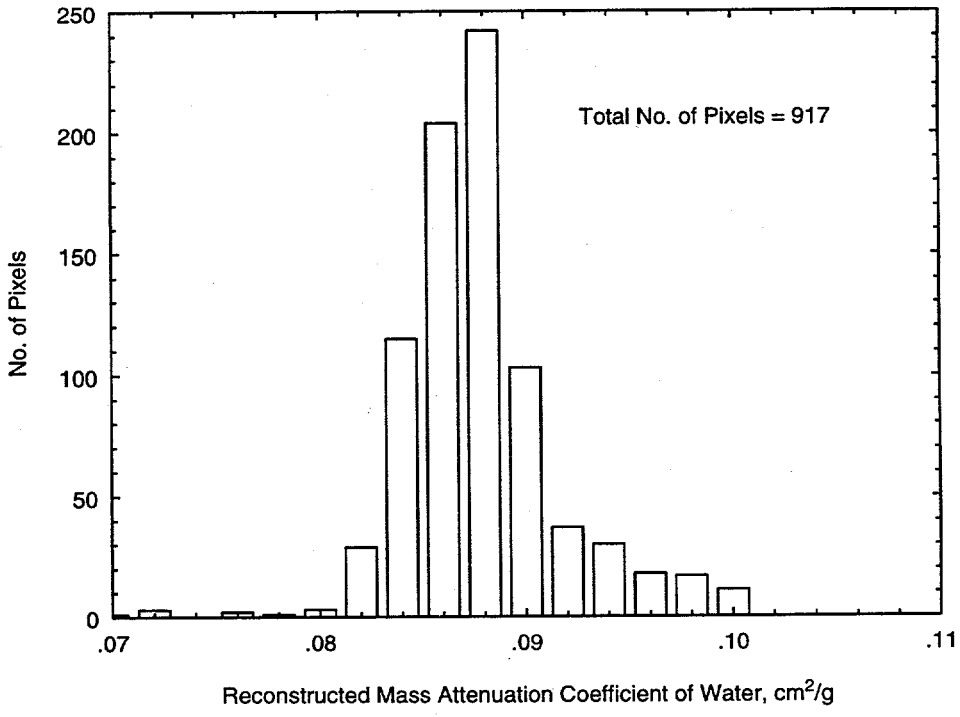

(b)

Figure 10: Spread of attenuation coefficients for water phantom reconstructed for (a) simulated data, (b) measured data

considered that any problem that produces a uniform error throughout a view is far less serious than that which produces a single bad projection in all the views (Shepp and Stein, 1977). The only means of overcoming this error is by identifying the detector in error and either replacing it or setting it right.

Measurement errors are also possible in systems making use of X-ray tubes as the source of radiation. It is assumed that X-ray tubes produce very small temporal and spatial variations in the output X-ray intensity. If there is some variation then the measured photon count rates for I_o would be a function of time and lead to errors in the computed transmission ratios. Often the X-ray output is monitored by a separate reference detector which rotates with the X-ray tube in a known constant geometric relationship. This, of course, only takes care of temporal variations and if there are spatial variations (the X-ray intensity is not isotropic) then the problem remains. The choice of a well designed X-ray tube that has a reasonably stable output is therefore critical in the design of an X-ray tomographic system. With gamma ray tomography the problem is not so critical especially if the isotope that is used has an extremely long half-life. The Cesium-137 source that is used for the scanner in our laboratory has a half life of 30 years. The unavoidable statistical nature of the emissions is taken care of by making use of a mean photon count rate (average of several samples) which is reproducible.

7 CT Scanner Design Process

In this section we present the steps involved in the choice of the design parameters for a CT scanner. For this we make use of the system in our own laboratory and the system designed by De Vuono (1979) at the Ohio State University, as examples. In the choice of the parameters, it is necessary to take into consideration a number of factors such as cost, source strength (dose rate), space constraints and mechanical considerations. All these factors are affected by the required spatial, temporal and density resolution. An increased spatial resolution calls for an increase in the number of detector channels. An increase in temporal resolution requires faster scanning capabilities, in which case the mechanical positioning devices need to be robust and the system needs to have the abilities to determine the positions of the scanning assembly accurately in a short period of time. All of these increase the cost of the required components. An increase in the density resolution requires an increase in the photon count rates and an increase in the number of views of the object. The former is limited by safety considerations, and the latter increases the scanning time which compromises the temporal resolution.

For the CT system in our laboratory the fourth generation scanning design was excluded

due to space and cost considerations. The number of detectors required for such a system would be at least a 100, and, the cost of the system increases dramatically with increase in the number of detectors. In addition, to accomodate test sections as large as 18 inches in diameter, the required space would be approximately 8' $\times$ 8', while we had a space constraint of 5' $\times$ 5'. The choice of the fan beam rotating source-detector system (third generation scanning) system meant that temporal resolution had to be sacrificed. We list the set of constraints and requirements for the design of the scanner below :

Spatial Resolution : 5 mm
Density Resolution : 0.05 g/cm^3
Scanning Time for a Column of 6" in diameter : 45 minutes
Maximum Allowable Source Strength : 100 mCi

The source-detector arc radius is generally set to be approximately twice the diameter of the largest test section to be scanned. In our case this radius worked out to 92.3 cm. The encapsulated Cs-137 source obtained from Kay-Ray Sensal, Mt. Prospect, IL has a fan beam angle of 40°. In order for the fan-beam to span the largest test section of 18" in diameter, the distance of the source from the center of the test section was determined to be 59.69 cm. This gives an average magnification factor M of 1.56. For a spatial resolution of approximately 5 mm the detector aperture can be computed using Eq. 10 in which the source width is 3 mm corresponding to diameter of the Cs-137 isotope. The aperture width that is computed is 7.5 mm. The aperture width that was chosen was, however, 5 mm, which means that our spatial resolution can be better than 5 mm. The height of the aperture was set to twice the aperture width following standard practice.

The number of projections (beams) per view that is required depends on aliasing considerations. To ensure adequate sampling of the flow domain it is, ideally, desirable that the successive beams in a view overlap or at least are close to each other. As was mentioned earlier, each detector was made to sample multiple beams by the use of a movable collimator that sweeps across the face of the detector array. The increment in the movement of the collimator was designed to be 0.5°. This corresponds to a linear movement of approximately 5 mm at the center of the test section which is close to the beam width at that location. We have demonstrated that this spatial sampling frequency results in no aliasing artifacts. The number of views required depends on the chosen number of projections per view and the required density resolution. Brooks and Di Chiro (1976) have established the criterion that the number of views m satisfy $m \geq n\pi/2$. For a column of 6" diameter the number of projections per view required is 26, and therefore the number of views in a scan of 180° is 49. This is true for parallel beam scanning for which the scans are obtained over 180°. With

fan-beam geometry however, it is necessary to scan over an angle of 180° + the fan-beam angle (Peters and Lewitt, 1977) (40° in our case). The number of views required is, therefore, approximately 60.

Having fixed the number of beams per view and the total number of views, one can now use the criterion for density resolution derived by De Vuono (Eq. 12) to calculate the photon count rates required and, hence, the required source strength. For a density resolution of 5 to 6 % with $m = 60$ and $n = 26$ for a 6" column full of water the required number of counts (computed from Eq. 12) is approximately 525. The photon counting time was selected to be 0.2 seconds, so that the total scanning time for a column of this size is about 45 to 50 minutes. The photon count rate required, therefore, is 2625 counts/sec. Since the maximum attenuation will be along the centerline of the test section, the source strength computations are made on the basis that this count rate is required along the centerline.

The measured count rate is a function of the source strength, the degree of collimation, the attenuation properties of the materials in the beam path, the sampling time and the efficiency of detection of the radiation sensors. The measured photon counts can be expressed as

$$N = S_o \tau \epsilon \Omega e^{-(\mu_p \rho_p (d_o - d_i) + \mu_w \rho_w d_i)} \tag{15}$$

where N is the number of photon counts in a given period of time (τ), S_o is the source strength expressed in photons/sec, ϵ is an overall efficiency factor for photon detection, Ω is the solid angle subtended by the detector aperture at the source and represents the effects of collimation, μ_p and μ_w are the mass attenuation coefficients (cm^2/g) of the pipe material and water respectively, and, d_o and d_i are the outer and inner diameters of the pipe. This expression is used for calculating the source strength, given the required photon count rate, the collimator dimensions, and the material properties of the pipe and the fluids involved in the experiment.

Since a point source emits radiation isotropically, only a fraction of the emitted photons can enter the detector aperture. This fraction is represented by the solid angle subtended by the detector at the source and can be defined as (Tsoulfanidis, 1983) as the ratio of the number of particles per second emitted inside the space defined by the contours of the source and detector aperture to the number of particles per second emitted by the source.

For the present geometry, in which the detector aperture is a rectangle with a width of $2a$ and $2b$, and the source detector distance is d, the solid angle is given by (Tsoulfanidis, 1983) :

$$\Omega = arctan \frac{ab}{d\sqrt{a^2 + b^2 + d^2}} \tag{16}$$

This expression holds for the situation where the source is on the axis of the rectangular aperture. Using this expression the solid angle is calculated to be 8.4×10^{-4}.

The detector efficiency gives the fraction of particles impinging on the detector that are recorded per unit time by the detector. It depends on the density and size of the detector material, the type and energy of radiation and the associated electronics. The simplest and most accurate method of measuring the detector efficiency is to record the number of photon counts in a given period of time for a calibrated source (Tsoulfanidis, 1983). If the obtained count rate is r (counts/sec), the equation for the efficiency is

$$\epsilon = \frac{r}{S\,\Omega\,\tau} \tag{17}$$

where τ is the sampling time. In an earlier section it was mentioned that in order to detect only those photons that deposit their complete energy in the detector (unscattered photons) the threshold voltage (above which the signal corresponding to a photon detection is considered to be for an unscattered photon) is set to a relatively higher magnitude. Thus, with a calibrated source the overall efficiency of detection was measured to be approximately 0.3 %. This value of the efficiency is low since we are gating in only on those photons that deposit their complete energy in the detector thereby minimizing the effects of Compton scattering. For a plexiglas column of 6" outer diameter, having a wall thickness of 0.25 inches, d_o and d_i are 15.24 cm and 13.97 cm, respectively. For a sampling interval of 0.2 seconds the required source strength is therefore approximately 100 mCi.

A similar case study has been presented by De Vuono (1979) for the design of a fourth generation scanning system. The assumptions made in that study was that the object is scanned over 180° and the number of views taken are equal to $m = \frac{3\pi n}{5}$ with n the number of beams per view equal to $d_i/\Delta x$, where Δx is the desired spatial resolution. The source ring and detector ring diameter are chosen to be twice and thrice the inside diameter of the pipe respectively. The physical detector area facing the source is $2.5\,\Delta x \times 5\,\Delta x$. The collimation used is different from the usual design having a single circular or rectangular beam. Instead the design of the collimator is such that the radiation impinging on an entire detector is broken up into several beams i.e., the collimator has a multi hole design. The effective detector area is therefore reduced, but an effective aperture width for use in Eq. 10 for calculating the achievable spatial resolution is not clear. It appears that the required spatial resolution is used in deciding on the number of beams per view. For a column with an internal and external diameter d_i and d_o, respectively, an expression for the number of

counts in terms of some of the parameters mentioned above is derived as :

$$N = \left(\frac{5\,\epsilon\,S\,\tau}{6\,\pi^2}\right)\left(\frac{\Delta\,x^3}{d_i}\right) e^{-(\mu_p\,\rho_p\,(d_o - d_i) + \mu_w\,\rho_w\,d_i)} \tag{18}$$

where τ in this case is the total scanning time defined as $\tau = m\,\tau_d$ where τ_d is the sampling time per beam. This equation, along with Eq. 12 for the density resolution, can be used to compute the required parameters for a given set of requirements and constraints.

The preset parameters are :

1. $d_i = 28.89\,cm$
2. $d_o = 32.38\,cm$
3. $\tau = 0.1 sec$
4. $\Delta\,x = 1\,cm$
5. $\sigma_\rho = 0.05\,g/cm^3$
6. $S \leq 1\,Ci$

The assumptions are :

1. 180° scan
2. 30 % collimator blockage
3. $\epsilon = 0.75$

It has to be noted that the assumed detector efficiency is very high in comparison to what was measured in our laboratory. We can only hypothesize that the thresholding used for discrimination between scattered and unscattered photons was low and consequently, the calculated strength of the required source will be low.

From the assumptions above,

$$n = \frac{d_i}{\Delta\,x} = 29 \text{ beams/view}$$

and

$$m = \frac{3\,\pi\,n}{5} = 55 \text{ views}$$

Note the relatively smaller number of beams per view as well as the number of views for a column of approximately 11.5 inches in diameter. This can be partially attributed to the relatively coarse spatial resolution that was desired.

The number of detectors in a fourth generation scanning system is dependent on the number of views. The number of views calculated above was for a 180° scan, hence, the number of detectors required in the entire circle is twice the number of views. Therefore the number of detectors required is 110.

The area of the detector is :

$$A_d = \frac{25}{2} \Delta x^2 = 12.5\, cm^2$$

and the actual area for detection after collimation is

$$A_a = 0.7\, A_d = 8.75\, cm^2$$

In comparison, the aperture area for a detector in our scanner is $0.5\, cm^2$. With $\mu_p\, \rho_p = 0.5678\, cm^{-1}$ (stainless steel pipe) and $\mu_w\, \rho_w = 0.0865\, cm^{-1}$ (for water) the calculated source strength is 3.17 Curies. It has to be noted that this source strength is high inspite of the low spatial resolution because the required temporal resolution is small. Since the design specification for source strength is violated, Δx was relaxed to $2\, cm$ and with all the other parameters unchanged the recalculated source strength is 198 mCi. With Δx increased to $2\, cm$, A_a is now $35\, cm^2$. Although this source strength was acceptable from design considerations, the resulting count rate of 4×10^5 cps is restrictive for most signal amplifiers. The spatial resolution was then relaxed to 3.5 cm ($A_a = 107.2\, cm^2$) and the density resolution to $0.06\, g/cm^3$. With the new parameters the new source strength required is only 14.7 mCi. The maximum count rate is now reduced to 9×10^4 cps. The reset values for the number of beams per view is 9 and the required number of views is 16. The total number of detectors now required is only 32. The required detector dimensions are 3.4" × 6.9" × 2". The total scan time being 0.1 sec, the scan speed works out to be 300 rpm.

From the above two examples it is clear that the design for the parameters of a CT scanner involves a number of compromises. In the first example the spatial resolution was given precedence over temporal resolution, while in the second case the temporal resolution was of prime concern. The density resolution in both cases was approximately the same, although in the second case it is not obvious if the desired density resolution was achieved in the scanner, since the number of views was only 16. It is also not clear what the effect of the multi-hole collimator design has on the spatial resolution of the system. The above design procedure is summarized in the following steps :

- Choose the type of scanning configuration desired. The general rule of thumb is that if temporal resolution needs to be high then the fourth generation scanning needs to be adopted.

- Set desired values for spatial, density and temporal resolution. An upper limit for the source strength needs to be determined based on safety considerations.

- Some details about the kind of source to be used need to be known at this juncture. Specifically, the source aperture and the fan-beam angle needs to be known.

- The source-detector and source-object distance must now be fixed. The magnification factor M can then be computed as the ratio of the source-detector distance to the source-object distance. Since the object (in our case a pipe of certain diameter) has a finite dimension, an average magnification factor can be computed using the distance of center of the pipe from the source as the source-object distance.

- The required detector aperture can then be calculated using the equation for the point spread function derived by Yester and Barnes (1977) (Eq. 10):

$$d_{eff} = \frac{1}{M}\sqrt{d_a^2 + (M-1)^2 s^2}$$

  where d_{eff} is set to the desired spatial resolution, and s the focal spot width.

- Based on the test-section diameter and the detector aperture the number of beams, n, in one view can be calculated. The number of beams has to be sufficiently large to avoid aliasing artifacts. The number of views, m, required can then be calculated using the criterion set by Brooks and Di Chiro (1976) :

$$m = \frac{3\pi n}{5}$$

- With the required density resolution and the established number of beams per view and number of views, Eq. 12 for the density resolution can be used to calculate the photon counting rate for a chosen sampling time.

- The required source strength can then be calculated using Eq. 15. The detection efficiency required here is best obtained by actual measurement using a calibrated source. The solid angle that is also required in this equation depends on the source-detector geometry and the collimator design and can be calculated using an appropriate expression provided by Tsoulfanidis (1983).